Bar-Ilan University

Proximity Effect in Insulating Granular System

Moshe Haim

Submitted in partial fulfillment of the requirement for the Master's Degree in the Department of Physics,

Bar-Ilan University

Ramat-Gan, Israel 2021

This work was carried out under the supervision of Prof. Aviad Frydman of the Department of Physics, Bar-Ilan University.

Acknowledgments

I would like to express my deep gratitude to my supervisor, Prof. Aviad Frydman, for embracing me into the lab under far-from-perfect circumstances and presenting me with the opportunity to carry this research under his guidance. Thank you for setting challenges, inspiring passion to the subject, and for pushing me in the right direction.

In addition, I would like to show my appreciation to all the lab members that took part in this work, from depositing samples to assisting with measurements, this meant a lot to me. Thank you, Ira Volotsenko, Arnab Roy, Roy Cohen, Yehudit Stein, Maayan Lahav and Avital Fried.

I would like to take this opportunity and thank my parents, Asher and Ora Haim for pushing me ever-forward and providing me with everything I needed to get here. Thank you for inspiring curiosity. I hope this will make you proud.

Last, but not least, I would like to end with a quote by the artist Calvin Cordozar Broadus, Jr (also known as Snoop Dogg), upon receiving his Hollywood star: `*I want to thank me for believing in me, and for doing all this hard work*`.

Table of content

Abstract

The superconductor insulator transition (SIT) in thin films draws a lot of interest in the field of condensed matter. mainly because it is a paradigmatic example of a quantum phase transition that can be tuned relatively easy and controllably by different tuning parameters. Although the SIT has been studied for decades, there are phenomena yet to be fully understood, one of which is the nature of insulating phase of the transition as there are many indications for the existence of superconductivity in this regime.

Studying superconductivity in the insulating phase via the `traditional` method of transport is futile since the divergence of resistance of the insulating parts of the system screens any signs of superconductivity that might exist. Tunneling measurements are also ineffective since they are limited to relatively high temperatures, close to the transition. In this work we demonstrate a different method to study the insulating phase of the transition via *the proximity effect* over a metal with a finite, measurable resistance.

The systems that we study in this work exhibit a granular behavior. The first one is structurally granular Pb that undergo the SIT as the grains couples. The second is an amorphous Indium-Oxide film that is morphologically uniform, however, electrically it consists of `droplets` of superconductivity in an insulating `ocean`, behaving effectively as granular. This behavior is described as `electrical granularity`. Both systems are coupled to a thin silver film having different disordered levels determined by the film`s thickness.

From this work we draw two main conclusions. First, even when the sample is on the insulating side of the transition, it can still `proximitize` a metal in the classical sense of reducing its resistance. The effect becomes larger as the sample is driven across the SIT. Second, and more interestingly, the proximity effect from a disordered superconductor on the insulating phase can induce insulating behavior into a highly disordered metal in a phenomenon we call `*Proximitized insulators*`. Traditionally the proximity effect is considered in the context of enhancing the conductivity of a metal. In our work, we show that inducing superconductivity to a disordered metal can decrease its conductivity. Additionally, we propose an explanation for the phenomenon based on the BTK model and Miller-Abrahams resistors network.

1. Theoretical background

1.1 Quantum phase transition

Classical phase transitions are driven by thermal fluctuations and characterized by a critical temperature Tc. At temperatures above Tc the system is in one phase and at temperatures below Tc the system is in a different phase. One example for a phase transition is the metal-superconductor transition. Above a certain critical temperature, T_c, the system is metallic and below it the system is superconducting. In contrast, a quantum phase transition [1] (QPT) occurs, by definition, at T=0. It is driven by quantum fluctuations and is controlled by a non-thermal tuning parameter g. At T=0 the transition occurs at a specific, well-defined value of $g = g_c$ which is called the quantum critical point (QCP). It goes without saying that T=0 is experimentally impossible. however, at any finite temperature this QCP is `smeared` into a critical quantum regime as shown in Fig. 1.1.

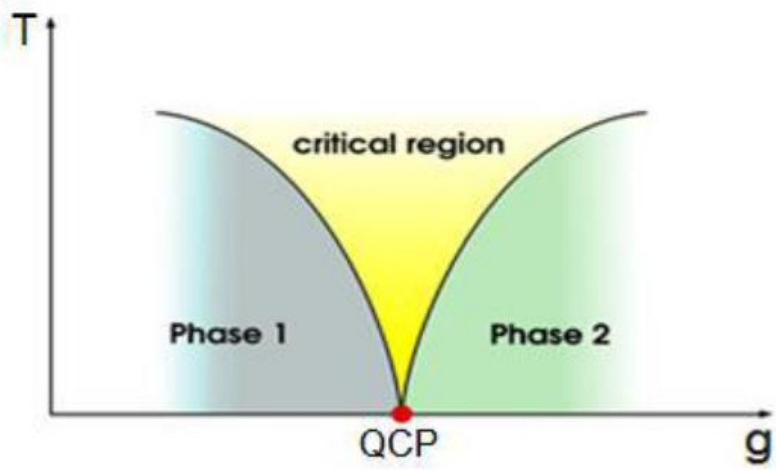

Figure 1.1: A schematic description of the QPT. At values of $g < g_c$ the system is in one phase, at $g > g_c$ the system is in another phase. At any finite temperature there is a critical quantum regime instead of a single point.

The quantum critical regime is characterized by quantum fluctuations of the two phases. Phase transitions are accompanied by a divergent correlation length and correlation time. The latter implies the existence of a frequency ω that is associated with the transition [2]. This frequency defines the energy scale of the quantum fluctuations ($\hbar\omega$), which should be compared to the thermal energy K_bT. If $\hbar\omega \gg K_bT$, the system is governed by quantum fluctuations. An example for a QPT is the superconductor-insulator transition (SIT) which is the main topic of this work.

1.2 The Superconductor-Insulator Transition

Superconductivity *per se* is well understood in a perfect lattice. It is described by the BCS theory [3], named after the physicists that have proposed it in 1957– Bardeen, Schrieffer and Cooper. One key aspect of this theory is the description of a mechanism that yields effective attraction between two electrons mediated by a phonon. This attraction causes the system to condense into a macroscopic state of a superconductor, in which the charge carriers form coper pairs. Further work by Anderson, extended the theory and predicted that superconductivity can exist even in 'dirty' superconductors [4] with non-magnetic impurities as was verified experimentally for weakly disordered systems. Howeover, it was shown experimentally that a superconductor can transit to an insulating phase by increasing the disorder [5-8] or alternatively, by tuning other non- thermal parameters (g) such as the film's thickness [9-10], external magnetic field [11], gate voltage [12] etc. For example, Fig. 1.2 presents two systems that undergo the SIT. The first (Fig. 1.2a) is the evolution of the resistance vs temperature curves R(T) at different thicknesses of a Bismuth film deposited on a Ge wetting layer [13]. The Second (Fig. 1.2b) is the evolution of the R(T) curves of an InO sample for different degrees of disorder [14].

The nature of the insulating phase of the transition is not fully understood. Experimental evidence that will be presented later, points to the existence of superconductivity in this regime. Since up to date, most of the research of the SIT was carried thorough transport measurements, any attempt to observe superconductivity in the insulator phase using transport methods will be screened by the increasing resistance. Lately however, there are various new attempts to study the transition using different methods such as tunneling measurements [15], specific heat measurements [16] and the Nernst effect [14]. In this work we use a different tool to study this transition i.e., the proximity effect. We will focus on systems that exhibit a granular behavior and can be theoretically treated within the framework of the `Bosonic model` of the SIT.

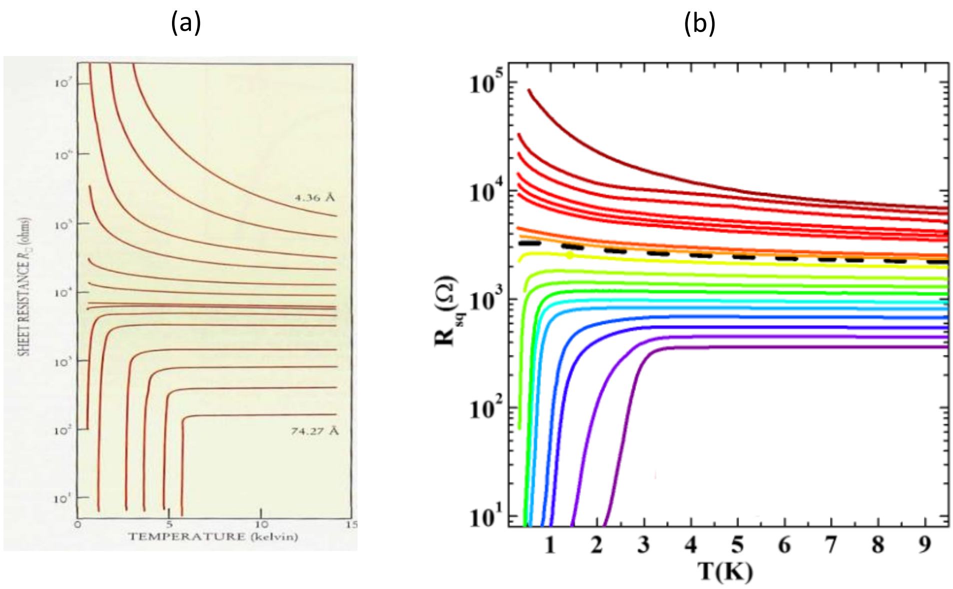

Figure 1.2: (a) Temperature dependence of sheet resistance for sequential layers of Bismuth deposited on a Ge thin film on an insulating substrate. Different curves correspond to different nominal thickness ranging from 4.36 Å to 74.27 Å [13]. (b) Temperature dependence of InO resistance for different degrees of disorder, achieved by thermal annealing [14].

1.3 The bosonic model

According to the Ginzburg-Landau theory, a superconducting wavefunction is described as complex function: $\psi = \psi_0 e^{i\theta}$ where ψ_0 is the amplitude and θ is the phase. The amplitude depends on the cooper-pairs density $\psi_0 = \sqrt{\rho_s}$, while the phase depends on the coupling between different parts of the system. Therefore, superconductivity can be suppressed by either phase or amplitude fluctuations. The bosonic model of the SIT is the theoretical description of systems that are dominated by phase fluctuations, hence global superconductivity can only exist if there is a global phase coherence. The model is based on cooper-pairs tunneling between different parts of the system via Josephson coupling [17]. A prototype system for this model is a granular system where each grain is a perfect bulk superconductor, having a random phase. The ability of cooper pairs to tunnel between grains is determined by two competing energy scales. The first is the Josephson energy $E_j = \frac{I_c \Phi_0}{2\pi}$, where $\Phi_0 = \frac{h}{2e}$

is the superconducting flux quantum and I_c is the critical current of the junction [18]. The second term $E_c = \frac{2e^2}{C}$ is the charging energy of each grain where C is the grain's capacitance. The ratio $\frac{E_c}{E_j}$ determines the ability of a cooper-pair to tunnel between grains and ultimately determines whether the system will be superconducting or insulating. If $E_j \gg E_c$ cooper pairs can tunnel easily between grains and the phase is well-defined across the sample. In this case global superconductivity is achieved. If the opposite is true ($E_j \ll E_c$) the pairs are localized and confined within each grain. In this case global superconductivity cannot be achieved.

From an experimental point of view, this model can describe systems with different `kinds` of granularity. The first is morphological granularity that consist of real superconducting grains. This system can be driven across the SIT by varying the coupling between the grains, for example by adding a metallic layer between the grains [19]. The second kind is `electrical granularity` in morphologically homogenous materials. These materials are electrically defined by superconducting islands that are surrounded by an insulating ocean. As the coupling between islands increases, the system is driven towards the superconducting regime. Such samples behave effectively as a granular material despite them being morphologically homogenous. Both systems are described in detail in the following sub-chapters.

1.3.1 SIT in a discontinuous superconductor

The first kind of granular system that we address is a thin, discontinuous superconductor. One classic example for such system can be obtained when gradually growing a thin superconducting layer on an insulating substrate. Fig. 1.3a presents the SIT of an ultra-thin granular Pb film (see a schematic structure of such sample in Fig.1.3b). Each curve corresponds to a different thickness; the lower the curve the thicker the sample. It is seen that the thinnest samples exhibit a divergence of resistance as $T \rightarrow 0$. As the thickness increases the resistance gradually drops. This regime is characterized by broad `tails`. As the thickness further increased, the resistance exhibits a sharp `drop` to zero resistance, behaving as a bulk superconductor. One important feature of the Figure is a change in behavior that can be observed in each of the curve, even in the insulating phase, at 7.2K, which is the bulk T_c of Pb.

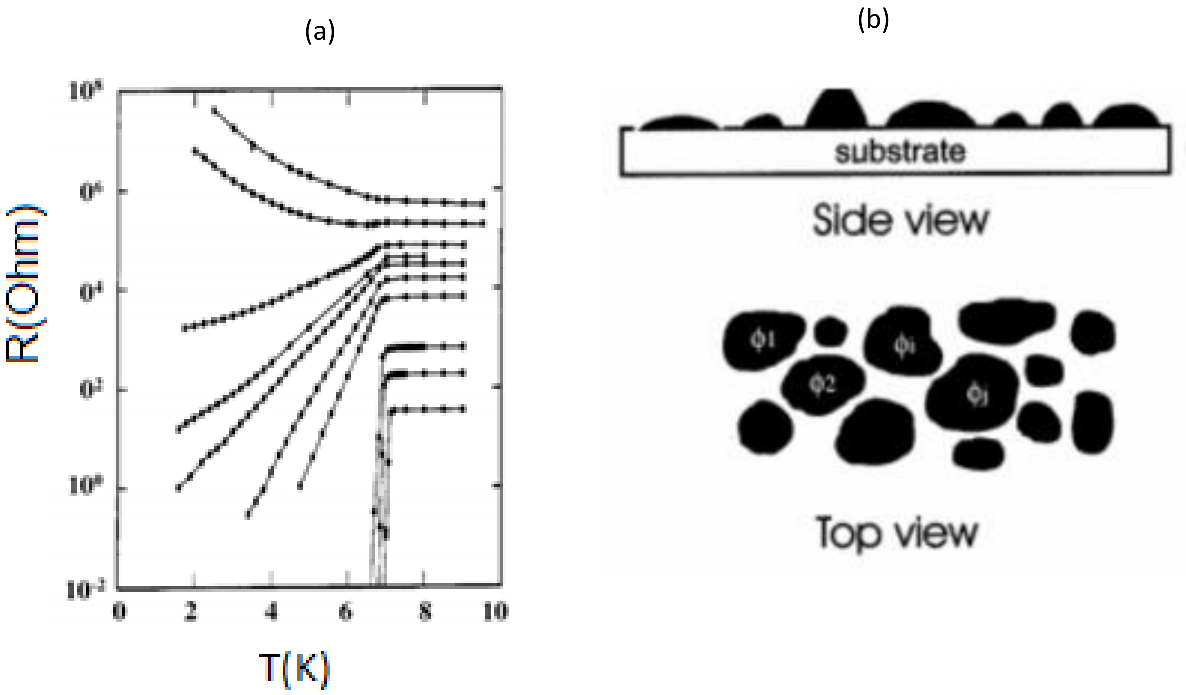

Figure 1.3: (a) Resistance Vs Temperature of a granular Pb film. Each curve corresponds to a different thickness (the lower the curve the thicker the Pb). (b) A side and top view of a microscopic scheme of this sample. Figure adopted from Ref. [9] and [20] respectively.

In order to explain this behavior, we shall consider the tunneling current between different parts of the system: Above the bulk T_c, the system can be considered as many metal-insulator-metal (M-I-M) junctions between which electrons tunnel in order flow across the sample. This leads to a lower resistance as the grains gets coupled, i.e. as the sample gets thicker. According to the bosonic model, below the bulk T_c each grain becomes a superconductor, which leads to an opening of a superconducting energy gap (Δ), making tunneling between islands harder at voltages below the gap [21]. In this case we can view the system as many S-I-S tunnel junctions in series and parallel [22], which yields an exponential increase in resistance as the temperature drops. On the other hand, below T_c some of the charge carriers form cooper-pairs and supercurrent can flow via Josephson tunneling between different grains. The overall behavior of the system will ultimately be determined on the coupling between the grains.

As the normal-state resistance is reduced by incrementally adding material, Josephson coupling improves (E_j increases) and the low-temperature behavior changes from insulating to superconducting [23]. This is manifested in Fig. 1.3a, for thick films (lowest curves) the grains are well-coupled ($E_j \gg E_c$) and cooper-pairs can tunnel between different parts of the system, hence a global phase coherence is maintained resultsing in a superconducting behavior. For the thinnest films (upper curves) it is seen that as the temperature decreases, the resistance increases exponentially, i.e. an insulator phase. In this case, inter-grain tunneling is less probable compared to a single electron tunneling above T_c. For intermediate thicknesses, E_c and E_j are of the same magnitude. This regime is characterized by long and broad `tails`, some of the curves appear to be reaching zero resistance where in others it is not clear whether it will happen. This gradual decrease makes it hard to define a critical temperature for the system.

In bulk superconductors, the formation of cooper-pairs and the observation of global superconductivity occurs at the same temperature - T_c. In a granular system however, this is not the case and one can define two temperatures: one is the temperature of cooper-pairs formation - T_ρ and one is the formation of global superconducting phase across the sample - T_ϕ. Applying this to Fig. 1.3 one can see that T_ϕ can be equal to the bulk T_c (as in a BCS superconductor), or it can be lower or even zero (as seen in the intermediate curves of Fig. 1.3a). This model allows the existence of local superconductivity even in the insulating phase of the transition. This claim is supported by different experimentas. For instance, tunneling measurements of the energy gap, Δ, have been performed on both sides of the SIT in thin Pb films [23-24]. The experiment showed that in granular Pb the energy gap does not vanish, and that each individual grain is able to support superconductivity, with bulk values of T_c and Δ [23]. Fig. 1.4 presents tunneling measurements of two Pb granular films, one is highly insulating (dotted), the other is superconducting (solid line). The Figure shows that the density of states and the energy gap hardly change with the sheet resistance.

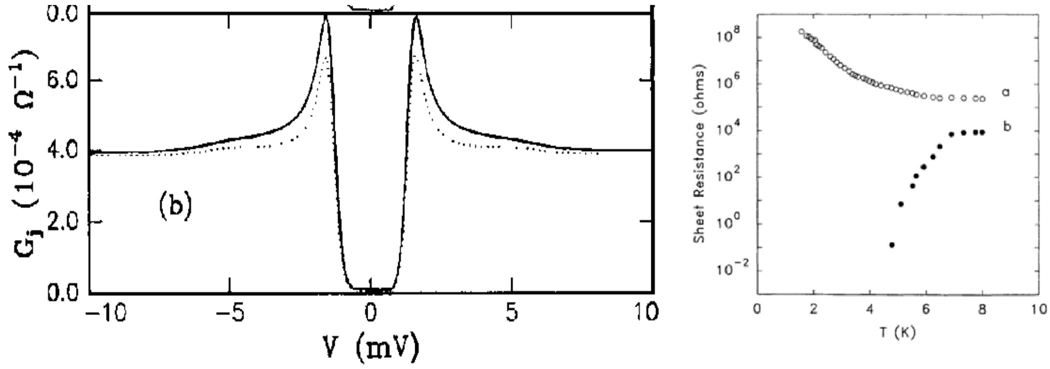

Figure 1.4 Left: Tunnel junction conductance as a function of voltage for a 17 $k\Omega$ (dotted) and a 375 Ω (solid) Pb granular films at 1.5K. Right: The resistance vs temperature of the same films. The $17k\Omega$ film is an insulator, while the 375Ω film is superconducting.

1.3.2 Electrical granularity of homogenous films

In superconducting elements, such as Pb or Sn, the study of the SIT in thin films was classified to either granular films or ultra-thin homogenous films. The two geometries gave rise to different results indicating two different types of SIT. Interestingly enough, a family of materials (for example amorphous Indium-oxide) that would be classified as \`homogenous\` from a morphological standpoint, exhibits electrical features that are similar to those of a granular system in the insulating phase, for example the presence of a finite superconducting energy gap. Fig. 1.5a shows temperature dependence of the resistance of two InO samples, one exhibits superconductivity while the other exhibits insulating behavior. Fig. 1.5b presents the normalized tunneling density of states of the two samples. The data indicates the existence of an energy gap in both the superconducting and the insulating phases.

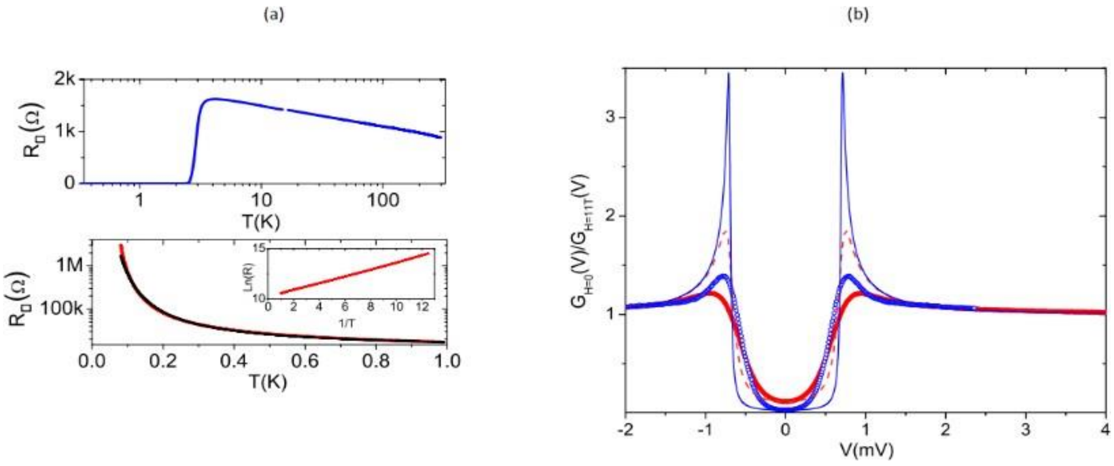

Figure 1.5: (a) Resistance vs Temperature of two amorphous InO samples, the top is superconducting while the bottom is insulating. (b) Normalized tunneling density of states (obtained at 1K) for the insulating sample (red) and the superconducting sample (heavy blue). Dashed red line and thin blue line are the BCS fittings of the insulator and superconductor, respectively. Figure adopted from [25].

The experimental data deviates from BCS theoretical expectation mainly in the suppression of the `coherence peaks`. Nonetheless, an energy gap still exists in both samples, indicating the existence of superconductivity in the insulating phase.

The results are explained in the framework of the `electron granularity` model [26], which introduces the concept of `droplets` or `islands` of superconducting fluctuations and is naturally consistent with the bosonic model. In more detail, as the system's disorder is increased, superconductivity does not disappear completely. Rather, T_c takes on a position-dependent range of values, meaning small reigns of superconductivity can still exist in a larger insulating `ocean`. The bulk T_c is determined from percolation considerations and eventually decreases to zero as the disorder is increased. On the insulating phase, transport is governed by tunneling between superconducting `droplets`. The deeper the system in the insulating phase, the rarer and sparser the droplets become. This make tunneling less probable, resulting in a stronger insulator. As the system is driven towards the SIT, the droplets grow in size and number, resulting in a better coupling, this leads to a lower resistance at low temperatures. When a large enough area of the system becomes superconducting, global superconductivity can be maintained and the system exhibits a superconducting behavior. This picture is analogous to the structural granularity case and can explain the similarities in the electrical features.

Tunneling measurements are a great technique to study the insulating phase since it allows us to study local superconductivity in the sample, even though the overall resistance is diverging. However, this method is ultimately limited, since it requires a barrier that is more resistive than the sample, i.e. $R_{Barrier} \gg R_{Sample}$. This condition limits this method to samples that are close to the SIT and at temperatures that are `not-so-close` to zero.

1.4 Giant magneto-resistance peak in disordered superconductors

The model of `electrical granularity` can also be utilized to explain the phenomenon of a giant magneto resistance peak, observed in disordered superconductors. Historically, old magneto-resistance (MR) measurements have shown a shallow peak in resistance at some magnetic field B_{max}, more recent measurements of amorphous InO film [27] have shown an enormous effect with the resistance value peaking at a few orders of magnitude higher than the resistance at $B = 0$. Fig. 1.6 presents the resistivity vs magnetic field of such InO film at various temperatures.

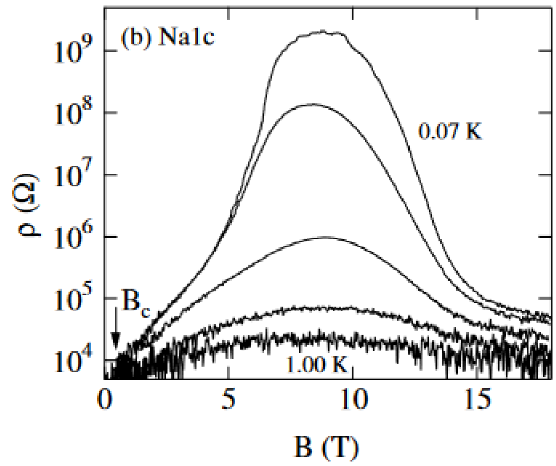

Figure 1.6: Resistivity vs magnetic field of an InO films at different temperatures, from top to bottom T=0.07K, 0.16K, 0.35K, 0.62K and 1.00K. [27]. The critical point of the B-driven SIT is indicated by the arrow.

Dubi, Meir and Avishai have proposed a model to explain this behavior [28] based on electronic granularity, assuming that applying a magnetic field decreases the size and concentration of the superconducting islands. Fig. 1.7 presents a schematic of the model.

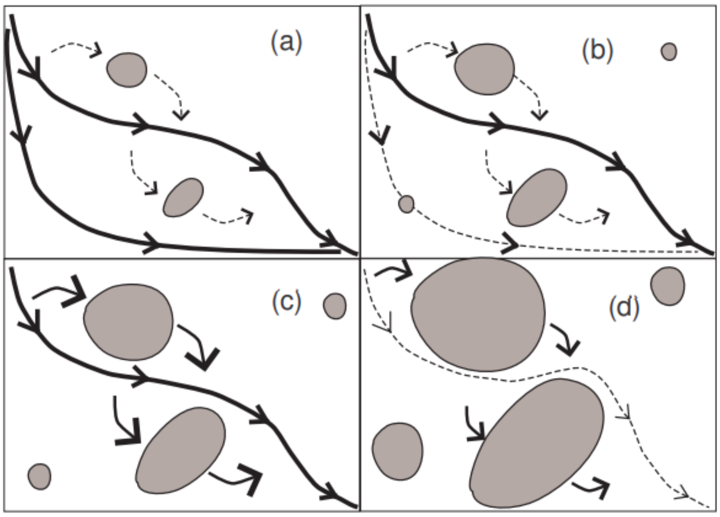

Figure 1.7: Schematic transport across a sample with different sizes of superconducting islands (grey). The solid black lines represent normal paths, and the dotted lines represents transport through superconducting islands. Figure adopted from [28].

Disordered superconductors, in this model, have two available trajectories for electron transport: those which follow normal, non-superconducting areas of the samples (`Normal paths`) and those in which electrons tunnel into a superconducting island via Andreev process (will be discussed in detail later). The normal path has some value of conductance, which may depend on the sample size, temperature, etc., and is assumed to be weakly affected by magnetic field. In the regime of strong magnetic field $B \gg B_{max}$, the islands are small and sparse, the charging energy is large and the main contribution to conductance is transport along normal paths (Fig. 1.7a). As the magnetic field decreases but still larger than B_{max}, the islands increase in both size and number, in this regime transport by normal paths is still favorable. However, some paths that were normal at higher fields becomes part of a superconducting island and hence unavailable for normal transport. Thus, resulting in a negative MR (Fig. 1.7b). Eventually, at $B = B_{max}$ (Fig. 1.7c), some islands are large enough so that the resistance through them is comparable to the remaining normal paths. At this point the resistance peaks, since as the magnetic field is further decreased (Fig. 1.7d), the number and size of the superconducting islands increases to the point that a larger enough fraction of the sample is superconducting, and transport through it becomes favorable compared to the normal paths. At the critical fields B_c the islands percolate through the systems, yielding a superconductor-insulator transition.

1.5 The Proximity Effect

The proximity effect [29] is the mutual effect between a superconductor and a `normal` (non-superconducting) metal that are in good electrical contact. Consider an interface between a superconductor and a normal metal. Far from the interface, in the superconducting regime, the superconducting order-parameter amplitude, Ψ_0, has a finite value while deep in the metal it is zero (since there are no cooper-pairs). The proximity effect asserts that the amplitude cannot change abruptly at the interface but rather varies smoothly, resulting in two consequences (as sketched in Fig. 1.8): First, the order-parameter amplitude has a finite value in the normal side extanding to a spatial distance of normal coherence length: $\xi_N = \sqrt{\frac{\hbar v_F l}{6\pi K_b T}}$ where l is the electronic mean free path, and v_F is the Fermi velocity. This implies that Cooper pairs leak into the non-superconducting region, where they exist with a finite lifetime before they are broken [30] with a decay length ξ_N. If the metal thickness is smaller than ξ_N, superconductivity can penetrate the entire metal. This is known as the `classical proximity effect`. Conversely, normal electrons leak into the superconductor, making it `weaker ` near the contact [31] and resulting in a suppression of superconducting parameters T_c and Δ over a distance of the superconducting coherence length $\xi_S = \frac{\hbar v_f}{\pi \Delta}$. This known as the `inverse proximity effect`.

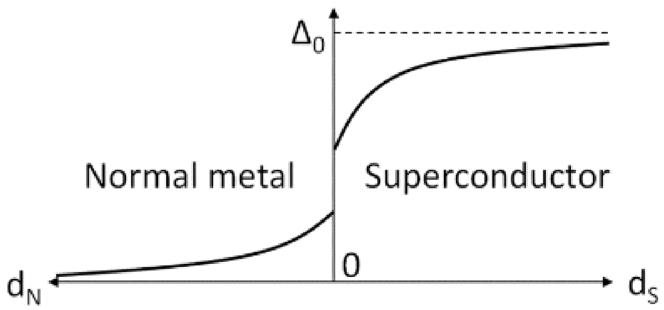

Figure 1.8: Evolution of the superconductor pairing potential Δ near an S/N interface. Δ_0 is the bulk pairing potential of the superconductor, (adopted from [32]). In general, there is a discontinuity in Δ at the interface, implying the interface is not perfectly transparent.

The proximity effect is influenced by three parameters: the decay length inside the metal, ξ_N, the superconducting coherence length, ξ_S, and the transmission between the layers t. From an Experimental point of view, proximity effect measurements require close to an ideal interface, so that the t is close to 1. This is only possible if the interface is very clean, with a minimal barrier between the materials. Another issue to consider is the mismatch between the Fermi velocities of the two materials. The higher the mismatch the larger the reflection [33]. These `obstacles` require a careful choice of metal and superconductor for such measurements. Using Ag as a metal with Pb as a superconductor is considered a good choice for proximity effect measurements [31].

1.6 Andreev reflection and BTK model

A microscopic view of the proximity effect and the conversion between single electron current in the metal to the supercurrent carried by cooper pairs in the superconductor was proposed by Andreev in 1964 [34]. Due to the existence of an energy gap in the density of states at the Fermi energy of the superconductor, the transfer of a single quasiparticle with energy below the gap ($E < \Delta$) across the barrier is forbidden [35]. An electron with energy below the gap impinging upon the interface can either be reflected, having no contribution to the net current, or it can pair with a second electron, adding a pair to the condensate in the superconductor, while reflecting a hole in a process called `Andreev reflection`. The process is schematically illustrated in Fig.1.9. If the electron carries ev_f of current (v_f is the Fermi velocity) then $2eV_f$ of net current flows through the interface since the returning hole carries $(-e)(-v_f)$ (current is conserved as the pair carries $2ev_f$ of net current in the superconductor).

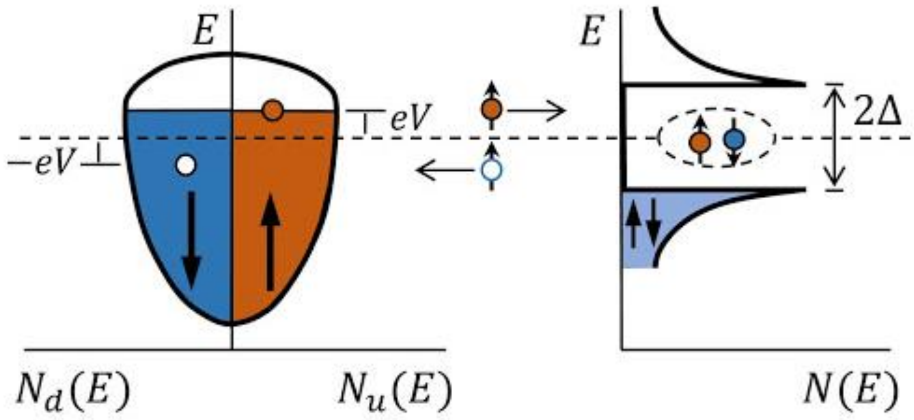

Figure 1.9: A schematic description of Andreev reflection. An electron (orange) impinging upon the interface is reflected as a hole (blue) while adding a pair to the superconductor.

At low voltages ($eV < \Delta$), electrons can only cross the interface via Andreev reflection, so for a pure Andreev process (no normal reflection), twice as much current flows compared to the case of the normal interface [36]. This can only occur when the interface is ideal ($t = 1$). If the interface is somewhat opaque, some of the electrons will be reflected, resulting in a lower conductance. As $t \to 0$, the conductance at voltages below the gap decreases to zero while gradually exhibiting coherence peaks, eventually resulting in a S-I-N tunnel junction.

The transition from a transparent to completely blocked tunnel barriers in S-N junctions was studied in detail in the BTK theory [36,37]. The theory introduces a dimensionless parameter Z which measures the barrier strength. This parameter is phenomenological and includes all sources for elastic scattering, including a physical barrier and the mismatch between the Fermi velocities of the two materials, that will result in some normal scattering even with no barrier present. The values of Z can range from 0, for a perfectly transparent metallic contact ($t = 1$), to ∞ for opaque barrier ($t = 0$). Fig. 1.10 presents differential conductance curves at T=0 for various barrier strength Z. At the top left curve the interface is completely transparent, indicating a pure Andreev process, while at the bottom right, the interface is very opaque, resulting in a S-I-N tunnel junction.

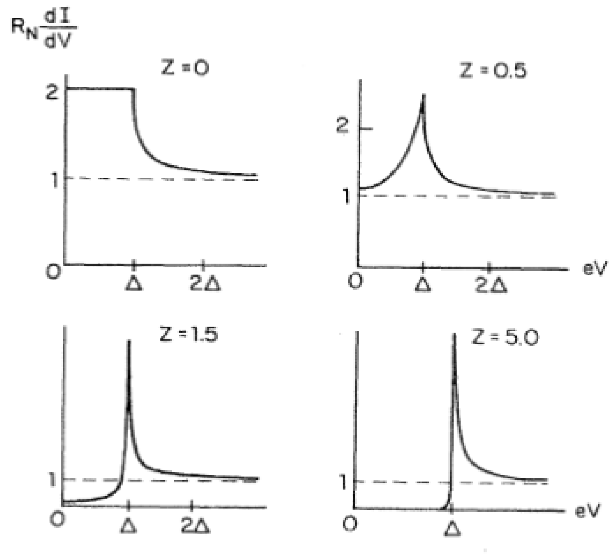

Figure 1.10: Differential conductance vs voltage for various barrier strength, at T=0. Adopted from [37].

2. Motivation

The study of the Superconductor-Insulator Transition (SIT) has been in the front of the condensed matter research both experimentally and theoretically for several decades, yet many aspects of the transition are not fully understood. For example, it became clear that in some systems, even in the insulating regime of the transition, local superconductivity or superconducting fluctuations can exist.

Past attempts to study the insulating regime of the transition had limited success. The traditional method of transport is problematic, since the diverging resistance is `screening` any superconductivity that might exist on a smaller scale. Tunneling measurements are more fruitful, but they are limited to samples that are close to the SIT at temperatures that are `not-so-close` to zero, in order to keep the barrier more resistive than the sample.

In this work, we propose a different method to study insulating samples by their effect over a metal, which has a finite, measurable resistance. This will be done by measuring *the proximity effect* signal between a metal in contact with a disordered superconductor on the insulating side of the SIT. If areas or fluctuations of superconductivity indeed exist, they should proximitize the metal. This makes the proximity effect a powerful tool that can be utilized to study samples deep inside the insulating phase.

Classically, the proximity effect is used to measure the mutual effect between a metal and a superconductor. We propose to study new areas of this effect, such as the proximity effect from weak superconductivity or from superconducting fluctuations. Furthermore, we wish to study the effect into a highly disordered metals on the verge of the metal-insulator transition. This may yield a more exotic effect of inducing an insulating behavior to the metal via the proximity effect.

3. Experimental methods

3.1 Sample preparation

In this work, the sample preparation is performed in three stages:

(I) six gold leads are deposited on an insulating SiO substrate by using a specifically designed shadow mask. The leads are 35nm thick, with an underlayer of 4nm of Ti that allows better adhesion of the gold to the substrate.

(II) Deposition of the normal metal for the proximity effect measurement. The obvious `candidates` for the normal metal are gold, silver and copper since all are non-superconductive and are considered a good choice for proximity effect measurement [31]. In order to be able to proximitize the metal film entirely, it is necessary that the thickness d will be smaller than ξ_N. Due to the need of a wetting underlayer (which is usually 3-5 nm) gold was ruled out although being the most inert of the three. Copper oxidizes easily which leads to poor electrical contact and low transmission through the metal-superconductor junction. Using silver minimizes both problems since it does not require an adhesive underlayer and the little oxide that it might form can be avoided by keeping the sample in a vacuum chamber or removed easily by plasma etching. Two thin strips of silver are deposited on the Ti/Au pads as illustrated in Fig. 3.1.

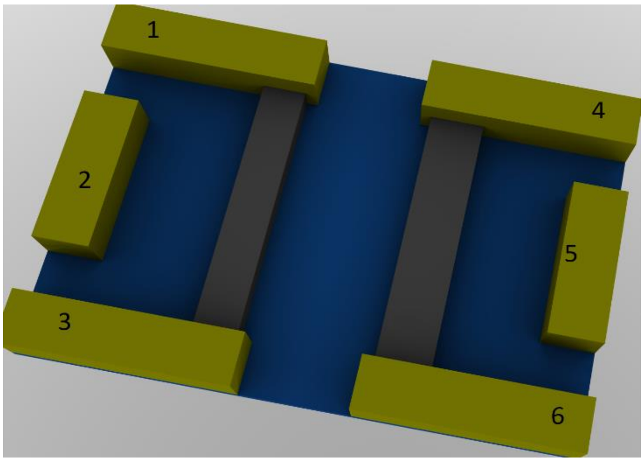

Figure 3.1: A schematic of the sample. Yellow and grey corresponds for gold pads and silver strips, respectively. Both are deposited on a silicon/silicon oxide substrate (blue).

Since part of the experiment focused on the proximity effect to a `dirty` metal, a silver sample that is extremely thin is required. The fabrication of such samples starts with the deposition of 10nm thick strips of Ag over the 6 gold pads configuration, which leads to strong metallic Ag. In order to bring the sample closer to the metal-insulator transition we use an argon plasma etching process to gradually thin the Ag strips. `Shaving` a metallic Ag strip resulted in more consistent and replicable samples than directly depositing thinner Ag. Due to their low thickness, even the slightest metal creep or oxidation will ultimately result in a dramatic change in properties, usually a large increase in the Ag resistance, making them too insulating and rendering them useless for us. Since the samples are not durable and have a short `shelf-life` of up to a couple of days after the etching, they are rushed into the evaporation chamber for the last step of the fabrication.

(III) Deposition of a superconductor on the substrate, covering the Ag, and connecting pads 2 and 5 of Fig. 3.1. This configuration yields two samples (Ag strips) for us to study simultaneously. Another advantage is the ability to have 4-probe resistance measurements of the superconducting material, using the silver strips as electrodes. Current is driven between pads 2 and 5, and the voltage is measured between pads 1 and 4 (or 3 and 6). This method eliminates the lead and contact resistance from the measurements, resulting in a precise 4 probe measurement of the area of interest as shown in Fig. 3.2.

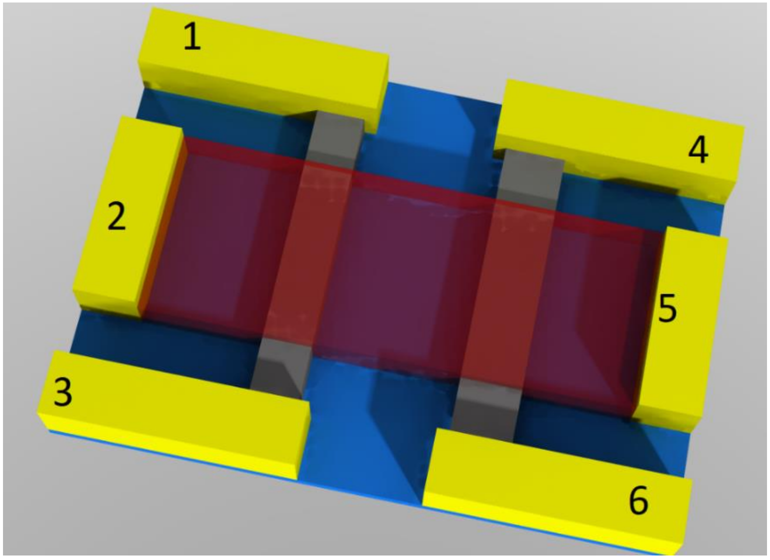

Figure 3.2: 4-probe measurement of the sample, driving current between pads 2 and 5 and measuring voltage between 1 and 4, resulting in a precise measurement of the resistance of the area in red.

3.2 Quench condensation

The first type of superconductors we study is a granular Pb. One experimental technique that can be used to fabricate a morphologically granular system that undergoes the SIT is `Quench condensation`, a thin film deposition technique in which a thin film is evaporated on a substrate held at cryogenic temperatures and ultra-high vacuum. It allows the study of extremely thin layers of a single sample as a function of thickness by *in-situ* sequential deposition. Since the sample is kept under extremely low temperature and pressure the evaporated atoms adhere to the surface and become rapidly immobile as they transfer their kinetic energy to the heat bath. When deposited on silicon, Pb creates nucleation sites that attract additional nearby atoms, resulting in a granular sample. On a silicon or glass substrate, the first stages of Pb deposition are non-continuous. Hence, the sample forms a collection of Pb grains within a vacuum matrix. In practice, Pb is deposited from a home-made `boat`, consisting of a tungsten wire that is spiral-shaped and connected to two electrodes (Fig. 3.3). A small piece of Pb is placed inside the cone and the setup is then inserted to a vacuum chamber and connected to a current source. Gradually increased current is driven through the boat heating the tungsten up to the point that Pb melts. This ensures that the Pb pallet will not fall when handled and inserted to the measurement apparatus.

Figure 3.3 The home-made evaporation boat. Tungsten wire is connected to two out of four available electrodes. The wire is spiral-shaped and a ball of Pb is placed on it.

Every stage of the measurement begins with a deposition stage at cryogenic temperatures. While this process is executed, the resistance of the Pb that is on the sample is constantly probed and this serves as a measurement of thickness that is calibrated against a well-known R-d curve. When reaching a required resistance, the evaporation is stopped. Throughout the entire process the temperature is kept below 10K.

When applying this technique, one must note that heating the substrate will make the evaporated material mobile and free to creep, this will lead to aggregation of small grains and the forming of larger disconnected islands. Exposing the sample to ambient pressure is also fatal since oxide layer is formed on the surface preventing the successive layers from connection (both physically and electrically). For these reasons the apparatus must remain cold and evacuated throughout the entire experiment. Fig. 3.4 illustrates a sample after the deposition of Pb.

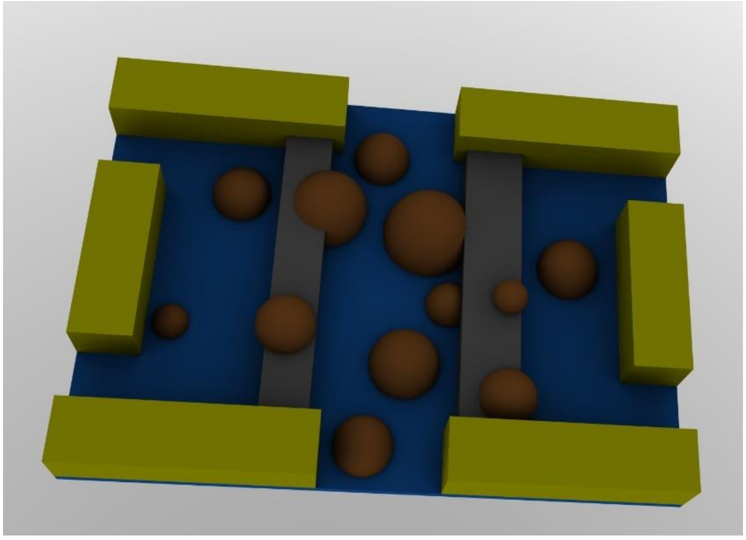

Figure 3.4: An illustration of a quench condensed sample. Grains of Pb (brown) are deposited randomly across the sample varying in shape and size.

3.3 Indium Oxide

The second type of superconductors we study is a 30nm thick, homogenous film of InO. Introducing pure oxygen gas to the deposition chamber at a certain partial pressure changes the stoichiometry by filling oxygen deficiencies [6]. This leads to a change in the carrier density n; the larger the oxygen pressure at the deposition, the smaller the carrier density is. If n is small, the ground state of the system will be an insulator, but if n is sufficiently large the samples will become superconducting at low temperatures. In practice, there is a correspondence between the resistance at room temperature to the behavior at low temperature. At room temperature, above ~$2k\Omega$ the sample will be insulting and below it, it will be superconducting at low temperatures. To drive the sample through the SIT, we thermally anneal the sample below $80°C$, while constantly probing the resistance. Once a desired reduction in resistivity is obtained the sample is cooled to cryogenic temperatures for further measurements.

The process of thermal-annealing is time-dependent; longer annealing time corresponds to a larger reduction of resistivity. However, the reduction slows down the more the sample is annealed, yielding a diminishing effect at long annealing times.

3.4 Measurements

The measurements in this work were conducted in a He_3 cryostat, capable of reaching 300mK and has a built-in 6T superconducting magnet. At each step of the experiments, two main types of measurement were performed using a well-known, standard technique:

1) R(T) measurements were taken using a standard 4-probes technique. The apparatus is heated to 10K by an on-board hearer, then, the resistance is continuously probed as the temperature is gradually decreased back to the base temperature.
2) Differential resistance-$\frac{dI}{dV}$ vs V measurements were taken by applying a bias DC current that is linearly swept in increasing steps. In addition, a small, sinusoidal AC current is added, and the response is measured in both the AC and DC channels, from which we extract the differential conductivity.

Occasionally, additional measurements were taken under magnetic field or at different temperatures, before driving the system one step further across the SIT by either quench condensation or thermal annealing.

4 Results

4.1 Ag characterization

First, we analyze the effect of disorder on the low-temperature behavior of silver. At low disorder we expect a metallic behavior i.e., a decrease in resistance with lowering temperature. At higher disorder we expect weak localization and an increase in resistance with lowering temperature. Fig. 4.1 presents the resistance vs temperature of 4 different Ag films with different disorder levels. Our measure of disorder is the room temperature resistance, R_{300K}, and for simplicity, each curve is normalized to its 10K resistance.

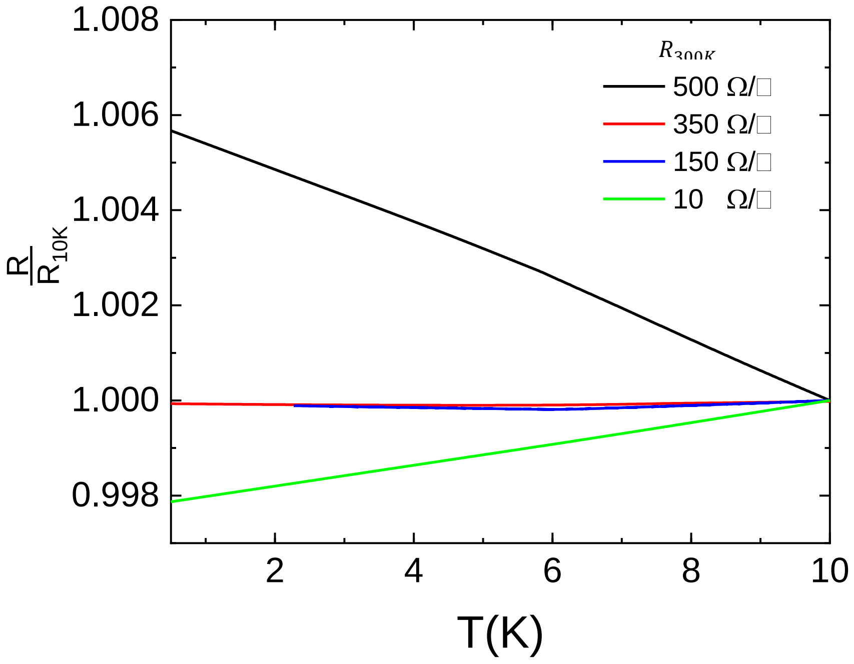

Figure 4.1: Resistance vs temperature of different Ag films, normalized to the resistance at 10K.

It is seen that at low disorder (green curve), the resistance decreases as the temperature is lowered, i.e., strong metallic behavior. At high disorder (black curve), the resistance slightly increases as the temperature is lowered. At a range of intermediate disorder (blue and red curves) the resistance is roughly constant. It is worth mentioning that in any case, the change in resistance is small within this temperature range, and does not exceed 0.6% increase.

4.2 Pb experiment

4.2.1 Resistance vs temperature

In the Pb experiment we have fabricated a $R_{300K} = 10\Omega_{\square}$ Ag film, on top of which, we quench condense granular Pb in incremental stages. At each step, the R(T) of both the Pb and the Ag/Pb bilayer were measured. Fig. 4.2 (a) presents the Pb curves and (b) presents the corresponding Ag/Pb R(T) curves with matching color. Note that panel b has the addition of a black curve which corresponds to the Ag prior to any Pb deposition.

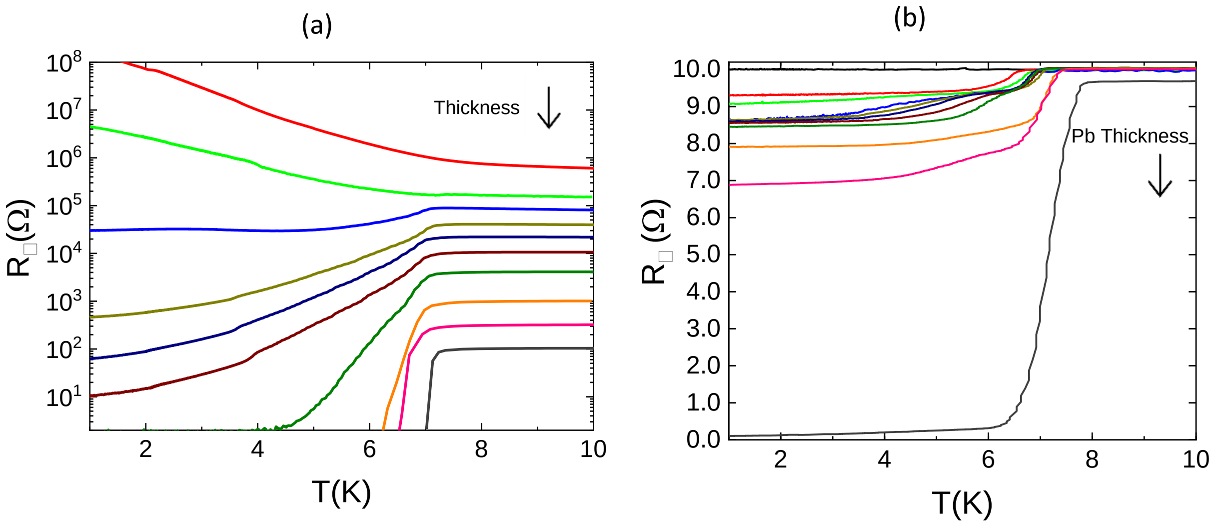

Figure 4.2: Transport measurements at different stages for: (a) Pb and (b) Ag. The curves at each stage have the same color.

It is seen that the Pb undergoes an SIT. For large enough thicknesses, the Pb is superconducting, with $T_c = 7.2K$. For low thicknesses, the Pb exhibits an exponential increase in resistance as the temperature is lowered. At intermediate thicknesses, the behavior is characterized by broad and long `tails`. Nonetheless, at every stage, a change in the resistance curves occurs at 7.2K which is the bulk T_c of Pb. This behavior is expected for granular Pb and has been discussed in detail at chapter 1.

The non-trivial part is shown in panel (b). As can be seen, even a small thickness of Pb, which is strongly insulating, affects the bilayer, causing the resistance to decrease at a critical temperature. To further emphasis this point, three Pb deposition stages were chosen and presented in Fig. 4.3. The figure compares the resistance of the Pb (red curves) and the corresponding Ag/Pb bilayer (blue curves).

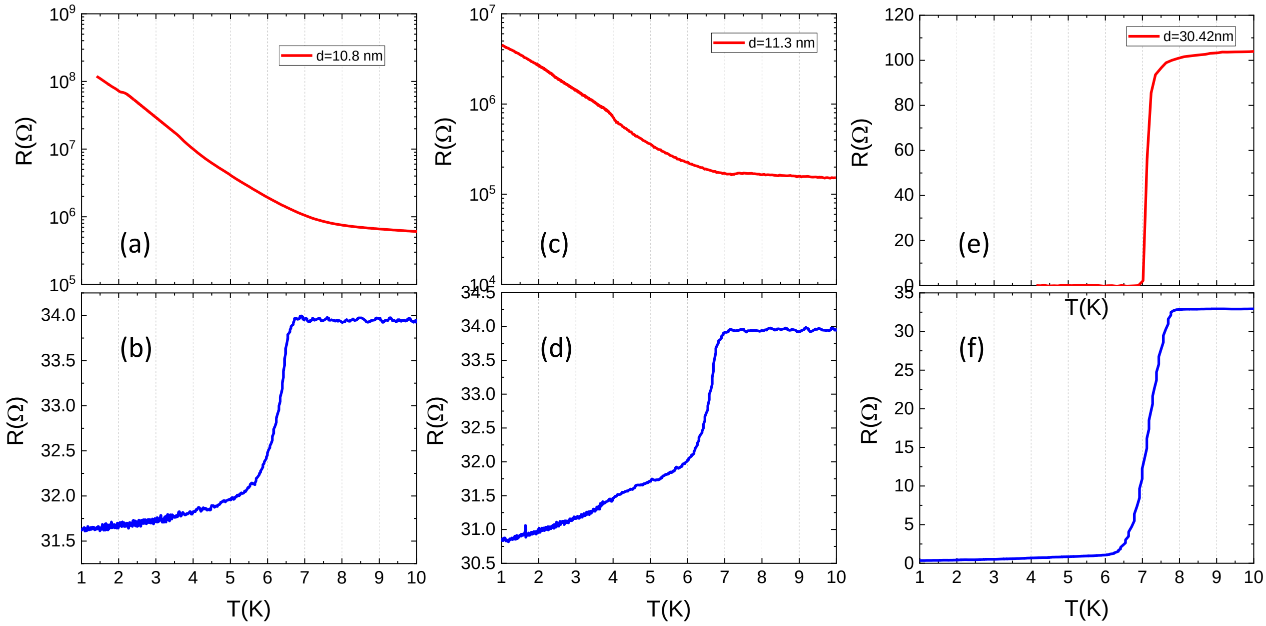

Figure 4.3: Selected deposition stages of the experiment. (a) and (b) are the first stage, (c) and (d) are the second stage, and (e) and (f) are of the 8th stage. The Pb thickness, d_{Pb} is calibrated from [16].

Panels (a) and (b) shows that even when the Pb is extremely thin and strongly insulating, it still induces superconductivity into the Ag. This is reflected in a reduction in the Ag/Pb resistance, as the temperature is lowered. As the Pb gets thicker, it proximitizes the Ag to a larger extent, causing a larger reduction in resistance, as can be seen in panels (c) and (d). At high enough thickness, the Pb becomes superconducting, in this stage the bilayer is also superconducting as shown in panels (e) and (f), probably due to the superconducting Pb shorting the bilayer. This effect that the Pb thickness has on the biis demonstrated in Fig. 4.4, which presents the percentage of reduction in the Ag resistance vs the Pb thickness in nm.

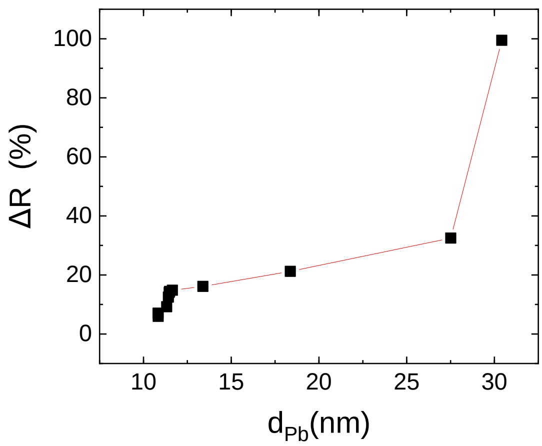

Figure 4.4: Ag resistance reduction vs the Pb thickness in nm.

4.2.2 Critical temperature

Another property that changes with Pb thickness is the critical temperature, T_c. We define the critical temperature for the Ag, as the temperature in which the resistance drops by 5%, compared to R_{10K}. Fig. 4.5 presents this T_c, as function of the Pb thickness d_{Pb}.

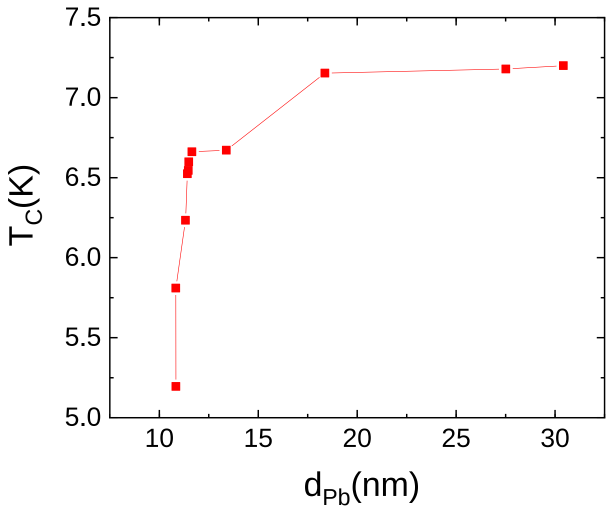

Figure 4.5: Ag T_c vs the Pb thickness. T_c is define as the temperature in which we measure a 5% reduction in the silver resistance.

As can be seen for a thin layer of Pb, the Ag/Pb T_c is lower than the bulk T_c of Pb (7.2K), as the Pb get thicker the effect diminishes and the critical temperature saturates at 7.2K.

4.3 InO experiment

This experiment differs from the previous experiment by two aspects:

1) The Pb has been replaced with InO that is uniform morphologically but believed to exhibit electrical granularity and is driven across the SIT by thermal annealing.
2) The relatively ordered Ag has been replaced by a disordered Ag.

We present data measured on three samples, each has an Ag film characterized by a different disorder level. The first sample (S1) has a resistance of $250\frac{\Omega}{\square}$, the second (S2) $220\frac{\Omega}{\square}$ and the third (S3) $150\frac{\Omega}{\square}$. Each pristine film is coupled to an amorphous InO_x that is driven through the SIT. Note that the Ag film resistance hardly changes between 10K to the base temperature (see Fig. 4.1).

4.3.1 Resistance vs temperature

`Fig. 4.6 shows the R(T) curves of the samples. The Ag/InO are presented in right panels alongside the corresponding stage R(T) curves of the InO in the left panels. Each Ag/InO_x R(T) curve is normalized to the resistance measured at 10K.

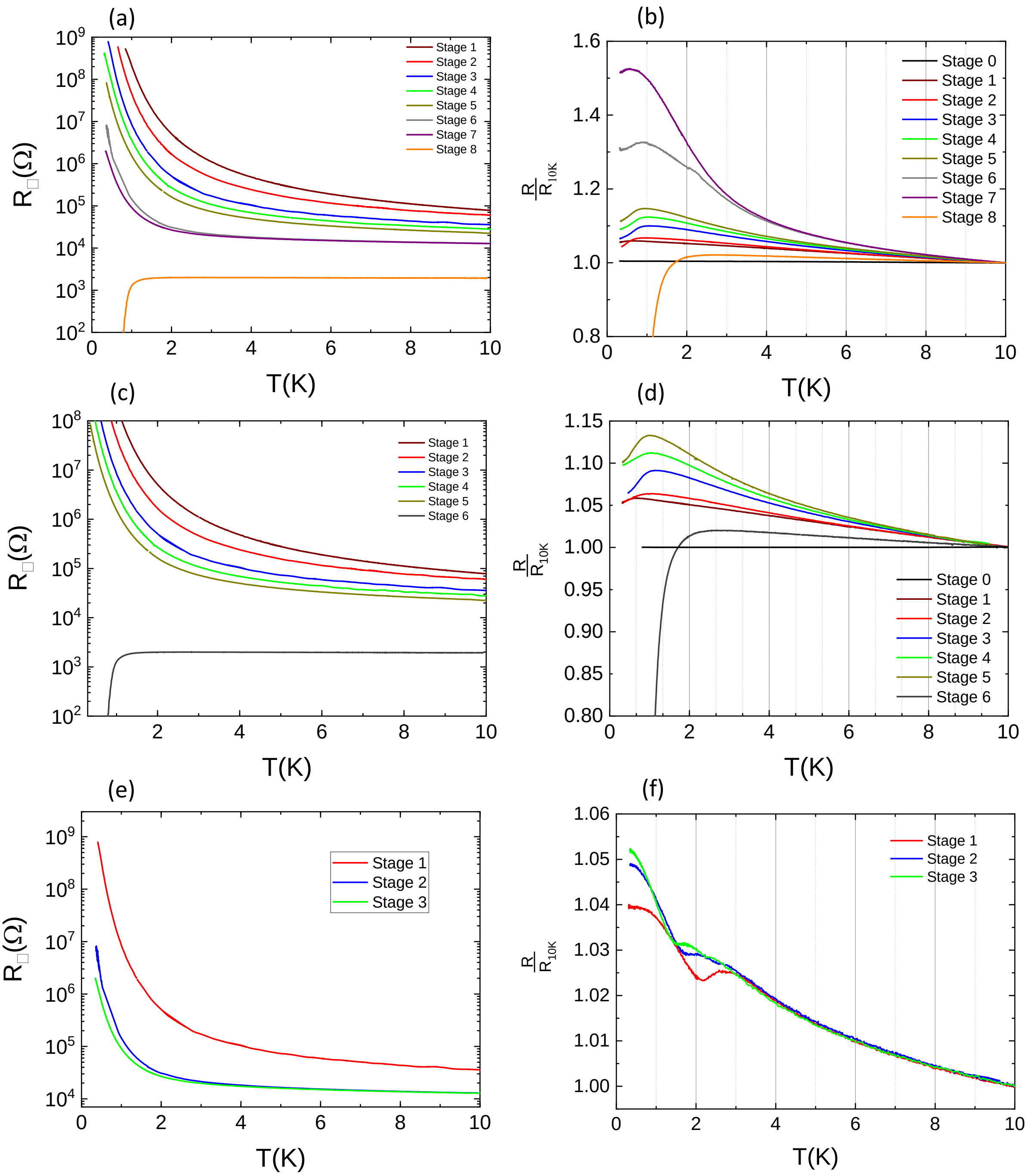

Figure 4.6: Resistance vs temperature of InO and Ag with different disorder levels. Panels a and b relate to S1, panels c and d relate to S2 and panels e and f relate to S3.

Contrary to the Pb experiment, for the first stages of InO annealing, instead of a reduction in resistivity of the bilayer as the InO is driven towards the superconducting phase, the opposite occurs, and the bilayer resistance increases. In S1 (panels a-b), where the Ag is the most disordered, we observed an increase of 6% for the most insulating stage. As the sample was driven closer the SIT the peak amplitude grew and reached over 50%. Sample S2 (panels c-d), for which the Ag was less disordered, exhibits the same trend, but to a smaller extent, 2-15% increase in peak resistance. Sample S3 (panels e-f), which had the least disordered Ag of the three, exhibited an even smaller effect of around 5% increase at most. This sample exhibits another feature; it has an additional, smaller peak in resistance at a higher temperature than the main peak. From this data we conclude that the peak increase in resistance depends on two parameters:

1) The Ag disorder level. The peak gets larger with Ag disorder.
2) The closeness of the InO film to the SIT. The peak is largest when the InO is close to the transition.

This is demonstrated in Fig. 4.7, which presents the increase in the bilayer resistance (in percent) vs the InO_x resistance at 1K. Note that here we have omitted the stage for which the InO is superconducting, since in this case the InO shorted the Ag.

.

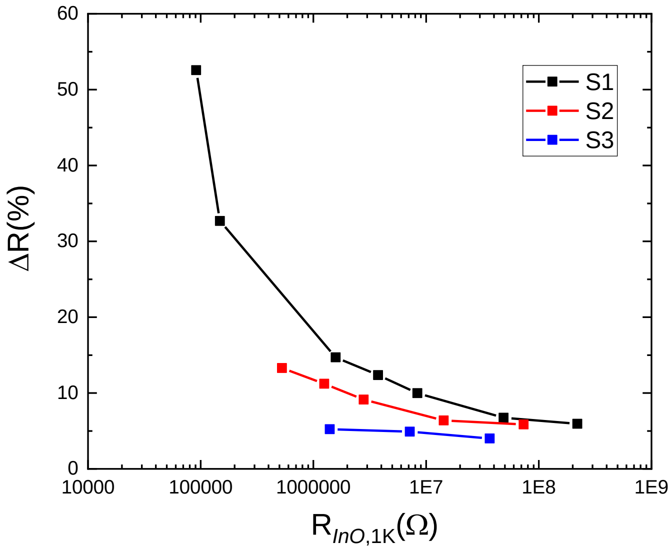

Figure 4.7: Ag resistance increase in percent vs of the InO resistance at 1K.

The data presented in Fig. 4.7 indicates that the closer the sample to SIT and the more disordered the metal, the larger the peak.

To further investigate this effect, in addition to R(T) measurements, we have conducted several differential conductivity measurements. The measurements resulted in a non-trivial behavior that are still under investigation.

4.3.2 Differential conductivity and energy gap

As stated, we have conducted several differntial conductivity measuremnts. Fig. 4.8 presents the differential conductivity, $\frac{dI}{dV}$, as a function of the voltage bias of the Ag/InO in sample S1 for the last three insulating stages (stages 5,6 and 7), at different temperatures. Each individual curve is normalized to the highest temperature measured (10K for stages 5 and 7, 8K for stage 6), for which we assume that no superconductivity exists.

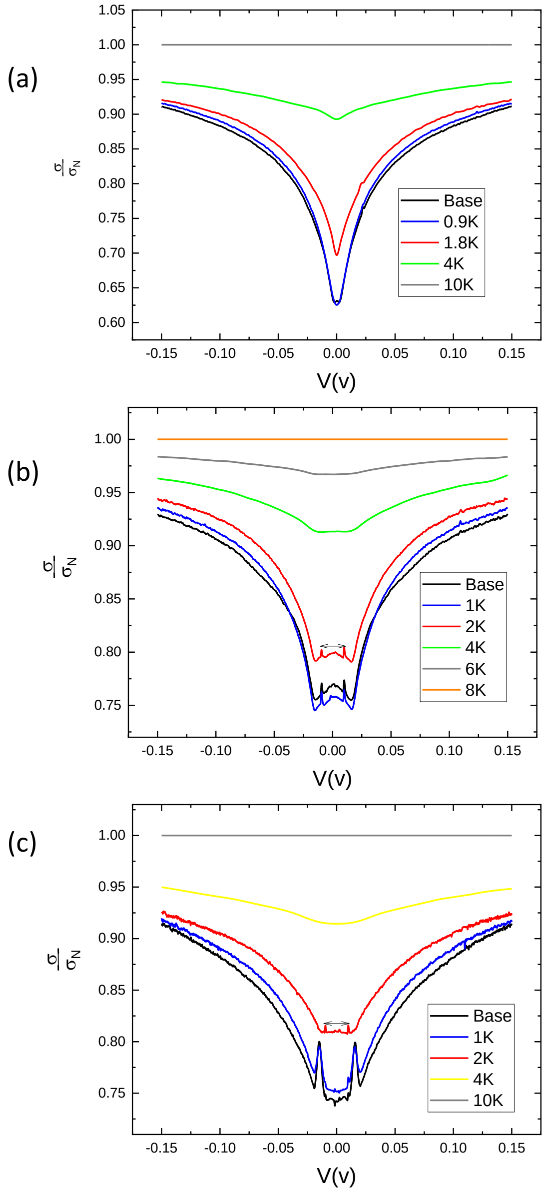

Figure 4.8: Normalized $\frac{dI}{dv}$ vs V of the Ag/InO bilayer at stages 5-(a), 6-(b) and 7-(c).

For stage 5, the data in Fig. 4.8 (a) shows zero bias conductance dip which vanishes with increasing temperature. This behavior is consistent with the zero-bias anomaly for weak disorder due to electron-electron interactions [38], which predicts that $\frac{dI}{dV} \propto \ln(V)$ and that at low bias, the conductance dip vanishes with increasing temperature. This is indeed confirmed in Fig 4.9.

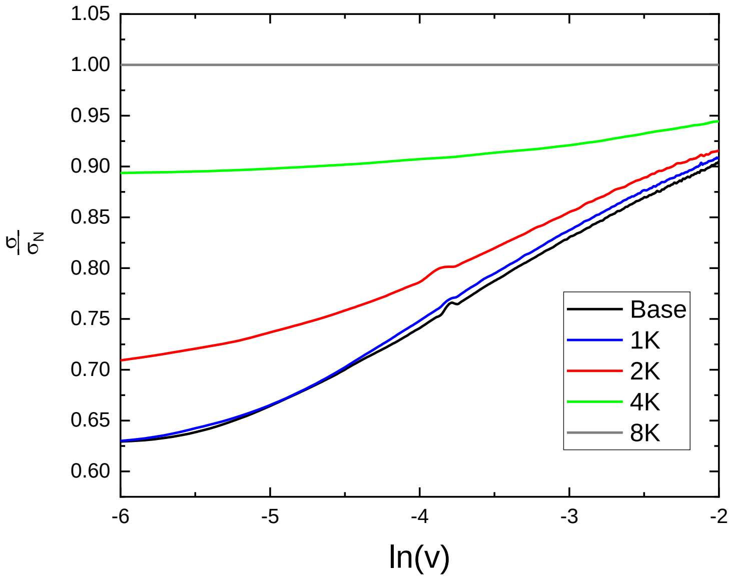

Figure 4.9: $\frac{dI}{dV}$ vs $ln(V)$ of S1 of stage 5.

Interestingly, for the next annealing stage (Fig. 4.8 (b)), additional non-trivial features appear. As can be seen, two symmetrical peaks appear on top of the general curve, marked by an arrow. After annealing the sample again the spacing between the peaks grow to 15.4mV for stage 7, compared to 9.8mV for stage 6.

Additionally, Stage 6 exhibits a small peak in conductance at zero voltage. This peak does not appear at stage 7, which exhibits a minimum of conductance. To further investigate the phenomenon, we have repeated the measurement of stage 6, in the presence of a magnetic field of 5.5T.

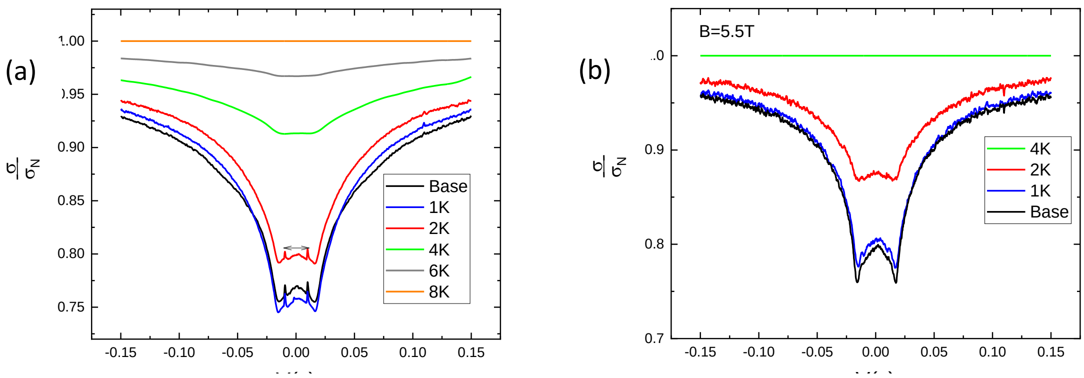

Figure 4.10: Normalized differential conductivity measurement of the Ag\\InO of S1, stage 6 at 0T (a) and 5.5T

As can be seen, the two symmetrical peaks completely vanish in the presence of the magnetic field, however, the peak at the center of the curve remains. These features resemble a kind of a superconducting energy gap, but the data is not conclusive. The subject is still under investigation as additional data is required.

5 Discussion

In order to explain the data measured in this work, we propose a qualitative model, that leans on Miller-Abrahams random resistor network [38] and the model proposed by Dubi, Meir and Avishai to explain the giant magneto-resistance peak in disordered superconductors [28] that was described in detail in chapter 1.4. This simple model is very useful in explaining most of the non-trivial features that we have observed.

5.1 Resistors network in a disorder metal

The Miller–Abrahams (MA) random resistor network [39] was introduced in order to study electron transport in disordered media. In their work, Miller and Abrahams assume that at low temperatures and low impurity concentration, conduction takes place by hopping of electrons from occupied to unoccupied localized sites. They map this problem into the form of a grid of nodes, connected by resistors of various resistivities, as sketched in Fig. 5.1. An electron traveling across such sample will take the path of least resistance. Hence paths including high resistors will not affect the total network resistance, since they will be bypassed by low resistance paths. This means that the overall resistance of a relatively disordered sample is governed by a few critical, low resistance resistors that are responsible for most of the conduction. Eliminating such critical resistors will have a dramatic effect on the resistance percolation network, leading to significant suppression of conductivity.

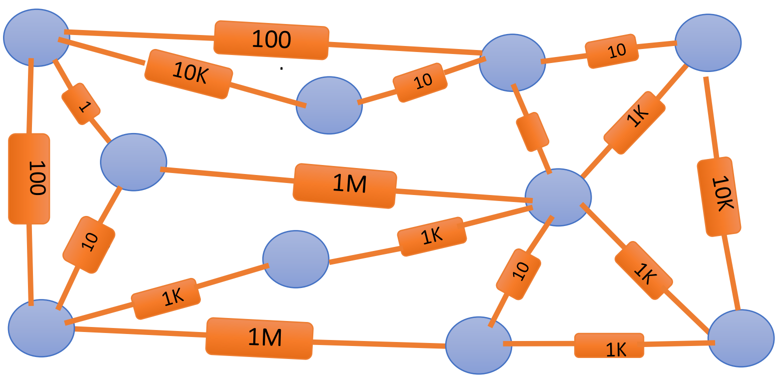

Figure 5.1: A sketch of a Miller-Abrahms random resistor network, used to describe conductance at disorder media.

When in contact with a granular superconductor (either Pb or InO_x), parts of the disordered Ag become superconducting due to the proximity effect. Applying this to the resistors network leads to areas of the network becoming superconducting, hence the network can be viewed as a resistors network which includes grains of induced superconductivity. Naively, one may expect that inducing superconductivity to the grid will enhance conductivity, but this is not always the case.

In order to understand how such including superconducting islands can result in either an increase or a decrease of resistance, we recall the physics of Andreev reflection and the BTK model, discussed in detail in chapter 1.6. As was explained, Andreev reflection is the mechanism of conversion of single-electron current to cooper-pairs supercurrent in an S-N junction that leads to enhancement of conductivity. Perfect Andreev processes requires` an ideal interface, i.e., the transmission through the junction should be close to 1. Our model leans on three elements from the BTK model: (I) The transmission through an S-N junction depends on the barrier strength Z, which can be a physical barrier such as an insulating layer or poor electrical contact. It can also be due to a large mismatch of the fermi velocities of the metal and the superconductor. (II) If the transmission is high, Andreev reflection is likely to occur, and we can expect an enhancement of conductivity. (III) If the transmission is low, i.e., Z is large, an electron cannot enter the superconductor via Andreev reflection, and will be reflected, leading to a suppression in conductivity. This means that if Z is large, inducing superconductivity yields a larger resistance, compared to the normal state.

The preliminary Ag/Pb experiment serves as a basis to test this hypothesis under near `ideal` conditions. It consists of a relatively low disorder Ag in contact with structural grains of Pb that are considered large enough to support bulk-like properties (see chapter 3.2). In addition to the low disorder of the Ag, the fermi velocities of Pb and Ag are relatively close: $1.39 \cdot 10^8 \frac{cm}{s}$ for Ag and $1.82 \cdot 10^8 \frac{cm}{s}$ for Pb. In this case one can expect, according to the BTK model, to have a strong Andreev reflection. Hence inducing superconductivity to the Ag will enhance the overall conductivity. An electron impinging upon a superconducting island is likely to undergo an Andreev reflection, since the transmission is large. This is consistent with the results of Fig. 4.2, in which we observed a reduction of the Ag resistance, below a critical temperature, even with the least amount of Pb deposition. As the Pb thickness increases, the influence of superconductivity (the improved conductance and the increasing T_c) increases. This experiment demonstrates that despite being insulating per-se, our Pb can proximitize and enhance superconductivity into a metal. Hence superconductivity can be induced in a metal, even from an `insulating superconductor`.

The InO experiment resulted in even more interesting results. Here we created the conditions for a reduced Andreev reflection, i.e., low transmission. This is achieved by two factors:

1) Using InO instead of Pb. This leads to a larger Z since InO and Ag have a larger mismatch of fermi velocities.
2) Using a relatively high disorder metal. We used three Ag samples, each with a different disorder. Increasing the disorder results in a lower coupling between the superconducting grains.

By reducing the transmission, we have managed to observe a non-trivial phenomenon which we call *`Proximitized insulators`*.

5.2 Proximitized insulators

The Ag/InO_x experiment consists of three samples with decreasing disorder, S1 S2 and S3. According to the Miller-Abrahams description of resistor network, we expect that more disordered samples have a wider distribution of resistors and are governed by a small amount of critical resistors. Since the probability for Andreev reflection is low (Z is large), an electron impinging upon an induced superconducting island will most likely reflect normally. This leads to current avoiding to enter the superconducting regions of the Ag sample, resulting in an increased resistance. This description is metaphorically like `puncturing` the Miller-Abrahms resistors network by inducing superconductivity, and the highest disordered Ag samples are expected to be affected the most, consistent with our results.

In addition, for each sample, the increase in resistance gets larger as the sample is driven towards the SIT. As each sample is driven towards the transition, the superconducting islands gets larger in size and density. for low density superconducting islands, the normal regions of the Ag can short the islands thus the effect is small. As we increase the proximitized area of the Ag there is a higher probability of proximitizing critical resistors which renders some of the `main` trajectories inaccessible and `force` the current to flow through lower conductance paths.

This model is similar to the description of the giant magneto-resistance peak suggested by Dubi, Meir and Avishai. In their model, they address an electrically granular material, in which the superconducting islands are suppressed by an external magnetic field. This leads to a giant magneto-resistance peak. The conductance through the medium is governed by the interplay between superconducting and normal trajectories. In our model the superconducting islands are induced and grow as the sample is driven across the SIT by disorder. The magnitude of the effect in our model is much smaller than Dubi, Meir and Avishai model, since we have addressed disordered metals that exhibit weak localization, rather than insulating, strongly localized systems. Nonetheless, in both cases inducing superconducting islands yields an increase of resistance that gets larger the more superconductivity is induced.

6 Conclusions

In this work we have presented a different view of the proximity effect. Traditionally, the phenomenon describes a superconductor the induces superconductivity into a normal metal. We have showed that the proximity effect extends much further.

First, we showed that the possibility of inducing superconductivity can be extended to samples on the insulator phase of the SIT. Second, and even more surprising, our work has shown a unique case that goes beyond the traditional understanding of the proximity effect, in a phenomenon we call *`Proximitized insulators`*. We showed that it is possible to induce insulating behavior to a disordered metal. We proposed an explanation based on Miller-Abrahms resistor network and the BTK model that explains how inducing superconductivity can result in an increase of resistance in a disordered medium, rather than an enhancement of conductivity.

This exotic effect can be used to the study the SIT in systems that are deep in the insulating phase, a regime that other conventional methods such as transport and tunneling measurement have been less fruitful. Attempting `to measure superconducting fluctuations in an insulating sample by transport is impossible, since the exponentially increasing resistance screens local superconductivity. Tunneling measurement require a barrier that is much more resistive than the sample, limiting the measurement to sample that are close to the transition and at relatively high temperatures. Our method is not limited in such a way. By coupling a film that is well within the insulating phase of the SIT to a normal metal, one can utilize the proximity effect and access transport and tunneling measurement of the coupled metal, regardless of how insulating the superconductor is.

This work can be considered a `proof of concept` that shows the vast span of possibilities that can arise from the proximity effect. Further research of this area is needed to complete the picture. Mainly, further investigation of the differential conductivity is needed. We have performed several measurements and the results seems to indicate the existence superconductivity, yet the data was inconclusive.

7. Bibliography

[1] Vasin, M. et al. Quantum-to-classical crossover near quantum critical point. Sci. Rep.5, 18600; doi: 10.1038/srep18600 (2015).

[2] Sondhi, S. L., Girvin, S. M., Carini, J. P. & Shahar, D. Continuous quantum phase transitions. Rev. Mod. Phys.69, 315–333 (1997).

[3] J. Bardeen, L.N. Cooper, J.R. Schrieffer, Theory of superconductivity, Physical review, 108(1957) 1175.

[4] P.W. Anderson, Theory of dirty superconductors, Journal of Physics and Chemistry of Solids, 11 (1959) 26-30.

[5] R. Crane, N. Armitage, A. Johansson, G. Sambandamurthy, D. Shahar, G. Grüner, Fluctuations, dissipation, and nonuniversal superfluid jumps in two-dimensional superconductors, Physical Review B, 75 (2007) 094506.

[6] D. Shahar, Z. Ovadyahu, Superconductivity near the mobility edge, Physical Review B, 46 (1992) 10917.

[7] B. Sacépé, T. Dubouchet, C. Chapelier, M. Sanquer, M. Ovadia, D. Shahar, M. Feigel’man, L. Ioffe, Localization of preformed Cooper pairs in disordered superconductors, Nature Physics, 7 (2011) 239.

[8] S. Poran, E. Shimshoni, A. Frydman, Disorder-induced superconducting ratchet effect in nanowires, Physical ReviewB, 84 (2011) 014529.

[9] A. Frydman. `THE SUPERCONDUCTOR INSULATOR TRANSITION IN SYSTEMS OF ULTRASMALL GRAINS`. Physica C 391 (2), 15, 189-195 (2003).

[10] V.F. Gantmakher and V.T. Dolgopolov, ' Superconductor-insulator quantum phase transition' Phys.-Usp.531 (2010).

[11] A. F. Hebard and M. A. Paalanen, Magnetic-field-tuned superconductor-insulator transition in two dimensional films, Phys. Rev. Lett. 65, 927 (1990).[12]

[12] C. G. L. Bøttcher, F. Nichele, M., et al , Superconducting, insulating and anomalous metallic regimes in a gated two-dimensional semiconductor–

superconductor array, Nature Physics volume 14, pages1138–1144(2018)Cite this article

[13] D. B. Haviland, Y. Liu, and A. M. Goldman, Onset of superconductivity in the two-dimensional limit, Phys. Rev. Lett. 62, 2180 ,1 May 1989.

[14] Arnab Roy, Efrat Shimshoni, Aviad Frydman, Quantum criticality at the superconductor insulator transition probed by the Nernst effect, Phys. Rev. Lett. 121, 047003 (2018).

[15] Sherman, D., Kopnov, G., Farber, E. et al. Tunneling Density of States of Indium Oxide Films Through the Superconductor to Insulator Transition J Supercond Nov Magn (2013) 26: 1473. https://doi.org/10.1007/s10948-012-2051-x

[16] Poran, Shachaf & Nguyen, Tuyen & Auerbach, Assa & Dupuis, Nicolas & Frydman, A & Bourgeois, Olivier. (2017). ARTICLE Quantum criticality at the superconductor-insulator transition revealed by specific heat measurements. Nature Communications. 8. 10.1038/ncomms14464.

[17] B. D. Josephson (1974). "The discovery of tunneling supercurrents". Rev. Mod. Phys. 46 (2): 251–254.

[18] J.M. Martinis, K. Osborne, Superconducting qubits and the physics of Josephson junctions, arXiv preprint cond-mat/0402415, (2004).

[19], C. G. L. Bøttcher1,5, F. Nichele, M. Kjaergaard, H. J. Suominen1, J. Shabani, C. J. Palmstrøm and C. M. Marcus, Superconducting, insulating and anomalous metallic regimes in a gated two-dimensional semiconductor–superconductor array NaturePhysics, 13, Aug 2018

[20]] L. Merchant, J. Ostrick, R. P. Barber, Jr. and R. C. Dynes, `Crossover from phase fluctuation to amplitude-dominated superconductivity: A model system,` Phys. Rev. B., 63, 134508, (2001).

[21] R. Dynes, J. Garno, J. Rowell, Two-dimensional electrical conductivity in quench-condensed metal films, Physical Review Letters, 40 (1978) 479.

[22] R.P. Barber Jr, R.E. Glover III, Hyper-resistivity to global-superconductivity transition by annealing in quench-condensed Pb films, Physical Review B, 42 (1990) 6754.

[23] R.P. Barber, Jr. L.M. Merchant, A. La. Porta, and R.C. Dynes, Tunneling into granular Pb films in the superconducting and insulating regimes, Physical review. B, Condensed matter, March 1994,

[24] J.M. Valles Jr., S. Hsu, R.C. Dynes, J.P. Garno, Electron tunneling studies of ultrathin films near the superconductor-to-insulator transition. Physica B 197 (1994)

[25] Sherman, D & Kopnov, G & Shahar, Dan & Frydman, A.. (2012). Measurement of a Superconducting Energy Gap in a Homogeneously Amorphous Insulator. Physical review letters. 108. 177006. 10.1103/PhysRevLett.108.177006.

[26] Kowal D., Ovadyahu Z., Disorder induced granularity in an amorphous superconductor. Solid State Commun. 90, 783–786 (1994).

[27] Superconductivity-Related Insulating Behavior, G. Sambandamurthy, L. W. Engel, A. Johansson, and D. Shahar Phys. Rev. Lett. 92, 107005 – Published 12 March 2004

[28] Yonatan Dubi, Yigal Meir, Yshai Avishai, Theory of Magneto-resistance of Disordered Superconducting Film, February 2006, Physical review. B, Condensed matter 73(5)

[29] Holm, R., Meissner, W. Messungen mit Hilfe von flüssigem Helium. XIII. Z. Physik 74, 715–735 (1932). https://doi.org/10.1007/BF01340420.

[30] Granqvist, C.G., Claeson, T. Superconductivity in ultrathin films II. Structure in tunneling curves. Phys cond Matter 18, 99–120 (1974). https://doi.org/10.1007/BF01456306.

[31] John Clarke. THE PROXIMITY EFFECT BETWEEN SUPERCONDUCTING AND NORMAL THIN FILMS IN ZERO FIELD. Journal de Physique Colloques, 1968, 29 (C2), pp.C2-3-C2-16.10.1051/jphyscol:1968201.

[32] G. Miao, Spintronics Driven by Superconducting Proximity Effect, SUPERCONDUCTORS–NEW DEVELOPMENTS, (2015) 127.

[33] G. E. Blonder and M. Tinkham, Metallic to tunneling transition in Cu-Nb point contacts, Phys. Rev. B 27, 112 (1983).

[34] A.F Andreev, ,1823(1964) [Sov.Phys.—JETP19,1228(1964)]

[35] B. Pannetier, H. Courtois, Andreev Reflection and Proximity effect , J. of Low Temp. Phys. 118, 599 (2000)

[36] G. Blonder, M. Tinkham, Metallic to tunneling transition in Cu-Nb point contacts, Physical Review B, 27 (1983) 112.

[37] G. Blonder, M. Tinkham, T. Klapwijk, Transition from metallic to tunneling regimes in superconducting micro constrictions: Excess current, charge imbalance, and supercurrent conversion, Physical Review B, 25 (1982) 4515.

[38] B.L. Altshuler A.G. Aronov, Zero bias anomaly in tunnel resistance and electron-electron interaction, Solid State Communications, Volume 30, Issue 3, April 1979, Pages 115-117

[39] A. Miller, E. Abrahams, Impurity Conduction at Low Concentrations. Phys. Rev.120,745–755 (1960).

תקציר

מעבר הפאזה מוליך על-מבודד במערכות דקות זכה לעניין רב בתחום החומר המעובה. זאת בעיקר בשל היותו דוגמא פרדיגמטית למעבר פאזה קוונטי, אשר ניתן לכוונון בצורה יחסית קלה וניתנת לשליטה, על ידי מגוון רחב של פרמטרים. על אף שהתחום נחקר כבר מספר עשורים ישנן תופעות שעדיין לא מובנות במלואן, למשל העובדה שישנן עדויות לקיום מוליכות-על גם בפאזה המבודדת.

ניסיונות למדוד מוליכות על בשיטות ה"מסורתיות" כגון מדידת התנגדות חשמלית הוכיחו עצמן כלא יעילות כאשר המערכת נמצאת בפאזה המבודדת, שכן ההתבדרות של ההתנגדות החשמלית ממסכת כל מוליכות-על מקומית. מדידות מנהור גם הן לא יעילות שכן הן מוגבלות לטמפרטורות יחסית גבוהות, ולמערכות הנמצאות קרוב למעבר הפאזה. בעבודה זו אנו מציעים דרך חדשה לחקור את הפאזה המבודדת על ידי שימוש ב"אפקט הקרבה" והשפעתו על מתכת בעלת התנגדות סופית וברת מדידה.

המערכות אותן אנו חוקרים הן בעלות אופי גרגירי. הראשונה מורכבת מגרגירי עופרת ועוברת את מעבר הפאזה מוליך על-מבודד על ידי שיפור בצימוד הגרגירים. המערכת השנייה מורכבת מאינדיום-אוקסיד אמורפי אשר מבחינה מבנית הוא "אחיד" ולא גרגירי, אך מבחינה חשמלית הוא מורכב מ"איים מוליכי על" המוקפים ב"אוקיינוס מבודד" בתופעה הנקראת "גרגיריות חשמלית". כל אחת מהמערכות הללו מצומדת לפס כסף בעל רמת אי-סדר שונה הנשלטות ע"י עובי הפס.

מעבודה זו הגענו לשתי מסקנות עיקריות: הראשונה היא שגם מערכת בפאזה המבודדת יכולה להשרות מוליכות על לתוך מתכת ולגרום לירידה בהתנגדות המתכת. אפקט זה גדל ככל שהמערכת עוברת את מעבר הפאזה. המסקנה השנייה, והמעניינת יותר היא שכאשר למתכת אי-סדר משמעותי, ניתן להשרות ממוליך העל התנהגות מבודדת לתוך המתכת בתופעה שאנו מכנים "מבודדי קרבה". לרוב, אפקט הקרבה מוזכר בהקשר של שיפור במוליכות החשמלית של מתכת. בעבודה זו אנו מראים שהשראה של מוליכות-על לתוך מתכת לא מסודרת יכולה לגרום לתוצאה ההפוכה ולירידה במוליכות. בנוסף אנו מציעים הסבר לתופעה, המבוסס על מודל BTK ועל רשתות מילר-אברהמס.

עבודה זו נעשתה בהדרכתו של פרופסור אביעד פרידמן מהמחלקה לפיזיקה, אוניברסיטת בר אילן.

אוניברסיטת בר-אילן

אפקט הקרבה במערכות גרגיריות מבודדות.

משה חיים

עבודה זו מוגשת כחלק מהדרישות לשם קבלת תואר מוסמך במחלקה לפיזיקה,

אוניברסיטת בר אילן

רמת גן, ישראל התשפ"א